MATHEMATICAL MODELING AND COMPUTING, Vol. 11, No. 4, pp. 1035–1045 (2024)

Blind image deblurring using fractional order derivatives and total variation: A Nash equilibrium approach

Berhich S., Moussaid N.

Hassan II University of Casablanca, LMCSA, FST, Mohammadia

(Received 14 September 2024; Revised 4 November 2024; Accepted 11 November 2024)

Fractional-order modeling represents a viable approach for addressing the inherent limitations of total variation in image deblurring tasks. This technique is achieved through the discretization of fractional derivatives and has demonstrated significant advancements in enhancing the quality of reconstructed images. Building upon the success of our previous work on blind deconvolution, where we utilized an image-based total variation to reduce the staircase effect, we analyze and test a novel blind deblurring model based on β-order fractional derivatives using the Nash game. This game employs the same type of players, each with their strategy to find an optimal solution, as defined in our previous work. Furthermore, we compare our proposed method with classical and fractional-order methods with different β parameters. Our numerical results demonstrate, that our method achieves higher effectiveness and better image quality compared to existing reconstruction methods.

Keywords: *blind image; deblurring image; fractional order derivatives; total variation; Nash equilibriums.*

2010 MSC: 91A05, 91A11, 91A12 **DOI:** 10.23939/mmc2024.04.1035

1. Introduction

The rectification of blurred images is a crucial aspect of image processing and computer vision, focusing on mitigating the adverse effects caused by various factors such as camera shake, defocus, or motion blur, which collectively reduce image sharpness. Image deblurring involves removing blur artifacts to restore a sharp representation of the visual content. Various methodologies have been proposed to aid in image restoration efforts, including nonlinear partial differential equations (PDEs) based on total variation [1–6], as well as non-local techniques [3,7,8]. Additionally, deconvolution, a widely employed technique, seeks to remove blur by modeling it as the convolution of the original image with a blurring kernel, which requires solving equations that describe this convolutional process. This study examines the degradation process inherent in image blurring through the following mathematical formulation:

$$z = k \otimes u + \eta. \tag{1}$$

In the context of image deblurring, we denote the observed image as z, the original image as u, and η represents the noise added to the blurred image. The blur is attributed to the kernel k, and the convolution operator $\otimes$ is employed. Total Variation (TV) serves as an established technique for image deblurring and restoration. The underlying principle of TV-based deblurring is to minimize the total variation of the image, thereby reducing the degree of blur while preserving essential image features like edges. This approach formulates the problem as an optimization task, wherein the objective is to find the image that minimizes the total variation subject to constraints. This optimization problem is typically resolved through the use of iterative numerical methods. A key challenge inherent in TV-based deblurring is the ill-posedness of the inverse problem, resulting in unstable solutions and artifacts in the reconstructed image. To address this issue, the Rudin–Osher–Fatemi (ROF) method introduces a regularization term, specifically the TV-L^2 regularization, into the optimization problem defined by

$$\min_u J(u) = \frac{1}{2}\|k \otimes u - z\|^2_{L^2(\Omega)} + \alpha \int_\Omega |\nabla u|\, dx. \tag{2}$$

The TV-L^2 regularization combines the total variation term with an L^2 fidelity term, which serves to balance the trade-off between deblurring and noise suppression. In this study, we focus on grayscale

images for simplicity. These images are considered as functions that map a rectangular domain $\Omega =]0, l[\times]0, L[$ into $\mathbb{R}$ (or $]0, 1[$), assuming they belong to the space TV-L^2. This regularization approach has demonstrated efficacy in enhancing the stability and improving the quality of the reconstructed image, rendering it a widely-utilized technique in the field of image deblurring and restoration. However, the ROF model frequently generates piecewise constant solutions, leading to an artifact commonly referred to as the staircasing effect. This artifact manifests as spurious edges or uniform regions in areas where smooth gradients are expected.

Consequently, Chan and Wong proposed an enhancement of the Rudin–Osher–Fatemi (ROF) method by introducing an additional regularization term that addresses both the image and the point spread function (PSF). This term is defined as follows:

$$\min_{u,k} J(u,k) = \frac{1}{2}\|k \otimes u - z\|^2_{L^2(\Omega)} + \alpha_1 \int_\Omega |\nabla u|\, dx + \alpha_2 \int_\Omega |\nabla k|\, dx, \tag{3}$$

where α_1 and α_2 are non-negative parameters. Moreover, Meskine et al. proposed a blind deconvolution method using Nash game, defined by

$$\min_{u,k} J(u,k) = \frac{1}{2}\|k \otimes u - z\|^2_{L^2(\Omega)} + \int_\Omega \alpha(x)|\nabla u|\, dx + \int_\Omega (1-\alpha(x))|\nabla k|\, dx, \tag{4}$$

where $\alpha(x) = \frac{1}{1+\gamma|\nabla G_\sigma \otimes z|^2}$ as an edge-stopping function, to control the speed of diffusion, where γ represents a threshold parameter, and $G_\sigma(x) = \frac{1}{2\pi\sigma^2}\exp\big(-\frac{|x|^2}{2\sigma^2}\big)$.

Fractional-order calculus is an extension of integer-order calculus, a discipline with a history spanning over 300 years [9–12]. Currently, three primary formulations exist for defining fractional-order differentiation: the Riemann–Liouville definition, Grünwald–Letnikov definition, and the Caputo definition [12]. Let β be a positive number assumed to be within the range of two consecutive integers, $n-1$ and n, such that $0 \leqslant l = n-1 < \beta < n$. The fractional β-order differentiation at a point $x \in \mathbb{R}$ is denoted by the differential operator $D^\beta_{[a,x]}$, where a and x represent the bounds of the integral over a one-dimensional (1D) computational domain, specifically lying between the two integers, $n-1$ and n.

The initial formulation for a derivative of general order β is referred to as the left-sided Riemann–Liouville (RL) derivative,

$$D^\beta_{\mathrm{RL}[a,x]} f(x) := \frac{1}{\Gamma(n-\beta)}\left(\frac{d}{dx}\right)^n \int_a^x \frac{f(\tau)\, d\tau}{(x-\tau)^{(\beta-n+1)}}. \tag{5}$$

Following that, the right-sided RL derivative and the Riesz-RL (central) fractional derivative are, respectively, presented as

$$D^\beta_{\mathrm{RL}[x,b]} f(x) := \frac{(-1)^n}{\Gamma(n-\beta)}\left(\frac{d}{dx}\right)^n \int_x^b \frac{f(\tau)\, d\tau}{(\tau-x)^{(\beta-n+1)}}, \tag{6}$$

$$D^\beta_{\mathrm{RL}[a,b]} f(x) := \frac{1}{2}\left(D^\beta_{[a,x]} f(x) + (-1)^n D^\beta_{[x,b]} f(x)\right). \tag{7}$$

The second formulation corresponds to the Caputo derivative of order β, defined as

$$D^\beta_{\mathrm{C}[a,x]} f(x) := \frac{1}{\Gamma(n-\beta)} \int_a^x \frac{f^{(n)}(\tau)\, d\tau}{(x-\tau)^{(\beta-n+1)}}. \tag{8}$$

Here, $f^{(n)}$ denotes the nth-order derivative of the function $f(x)$. Similarly, the right-sided derivative and the Riesz–Caputo fractional derivative are defined equivalently as

$$D^\beta_{\mathrm{C}[x,b]} f(x) := \frac{(-1)^n}{\Gamma(n-\beta)} \int_x^b \frac{f^{(n)}(\tau)\, d\tau}{(x-\tau)^{(\beta-n+1)}}, \tag{9}$$

$$D^\beta_{\mathrm{C}[a,b]} f(x) := \tfrac{1}{2}\big(D^\beta_{[a,x]} f(x) + (-1)^n D^\beta_{[x,b]} f(x)\big). \tag{10}$$

The third formulation corresponds to the Grünwald–Letnikov derivative of order β, defined as

$$D^\beta_{[a,x]} f(x) := \lim_{h\to 0} \frac{1}{h^\beta} \sum_{j=1}^{[\frac{x-a}{h}]} (-1)^j C^\beta_j f(x-jh), \tag{11}$$

where $C^\beta_l = (-1)^l \frac{\Gamma(\beta+1)}{\Gamma(l+1)\Gamma(\beta+1-l)}$.

Both the Riemann–Louville definition and the Caputo definition rely on the Cauchy integral formula, resulting in computational complexity. In contrast, the Grünwald—Letnikov definition can be transformed into a convolutional form during numerical implementation, showcasing enhanced adaptability to image signal processing. Therefore, this paper utilizes the Grünwald–Letnikov fractional-order definition to improve the effectiveness and efficiency of image deblurring. Numerous authors have proposed models based on fractional-order derivatives. In this paragraph, we highlight some of these works: Zhou and Tang [13] proposed a fractional-order total variation (FOTV) blind image restoration algorithm based on the L^1-norm using iterative semi-quadratic regularization to solve the problem. Zhang et al. [14] described a novel computed tomography reconstruction method that utilizes fractional-order total variation, considering more neighboring image voxels and adaptively determining corresponding weights to suppress the over-smoothing effect. Zhang and Wei [15] proposed a new variational model for image denoising based on fractional-order derivatives instead of the gradient of the image. They also provide a numerical algorithm for solving the model based on the discrete fractional difference. Zhou et al. [16] employed a fractional-order model that extends the integer-order total variation to reduce artifacts. Self-similarity is introduced as prior information because natural images usually exhibit texture features. The cost function is generated and solved using semi-quadratic regularization. Another group of authors suggested a method for blind restoration of motion-blurred images using fractional-order regularization and sparsity constraint. They utilized the split Bregman method to combine an iterative thresholding algorithm [17]. This paper aims to suppress the over-smoothing effects and preserve edges in image processing and restoration methods. For this reason, this paper is organized as follows: Section 2 presents the preliminaries, including fractional-order total variation using the Nash game proposed in Section 3. The experiments are demonstrated in Section 4, and the conclusion is presented in Section 5.

2. Preliminaries

2.1. Definitions and operators of Fractional-order total variation

The Grünwald–Letnikov definition. The Grünwald–Letnikov fractional-order derivatives, ∇_x^β and ∇_y^β, for an input image u of order $\beta \in \mathbb{R}^+$, are given by

$$\nabla_x^\beta u_{i,j} := \sum_{l=0}^{k-1} C_l^\beta u_{i-k,j}, \tag{12}$$

$$\nabla_y^\beta u_{i,j} := \sum_{l=0}^{k-1} C_l^\beta u_{i,j-k}. \tag{13}$$

Here, k signifies the number of neighboring pixels. Additionally, the discrete fractional-order gradient is denoted as $\nabla^\beta u = (\nabla_x^\beta u, \nabla_y^\beta u)^{\mathrm{T}}$.

Definition of the adjoint and divergence operators of FOTV. The adjoint operators for the fractional-order derivatives are defined as follows:

$$\left(\nabla_x^\beta\right)^{\mathrm{T}} u_{i,j} := \sum_{l=0}^{k-1} C_l^\beta u_{i+k,j}, \tag{14}$$

$$\left(\nabla_y^\beta\right)^{\mathrm{T}} u_{i,j} := \sum_{l=0}^{k-1} C_l^\beta u_{i,j+k}. \tag{15}$$

By applying these definitions to a vector function $p(x,y) = (p_1(x,y), p_2(x,y))$, we can derive the fractional divergence operator as:

$$\mathrm{div}^\beta p = (-1)^\beta \left(\nabla^\beta\right)^{\mathrm{T}} p = (-1)^\beta \left(\left(\nabla_x^\beta\right)^{\mathrm{T}} p_{i,j}^1 + \left(\nabla_y^\beta\right)^{\mathrm{T}} p_{i,j}^2\right). \tag{16}$$

2.2. Properties

Zang and Chen discuss a generalization of the Total Variation (TV) regularizer in [18], known as the fractional total β-order regularizer, and its associated mathematical properties within the β-bounded

variation space. The fractional total β-order variation of a function u is defined by

$$\mathrm{TV}^{\beta}(u) = \sup_{\mathbf{v}} \left\{ \int_{\Omega} -u \ \mathrm{div}^{\beta} \mathbf{v} \, dx \mid \mathbf{v} = (v_1, v_2) \in \left(C_0^1(\Omega, \mathbb{R}^2)\right)^2, \|\mathbf{v}\|_{L^{\infty}} < 1 \right\},$$

where $0 \leqslant l = n-1 < \beta < n$, $\|v\|_{L^{\infty}} = \max \sqrt{v_1^2 + v_2^2}$, and $\mathrm{div}^{\beta} v = \frac{\partial^{\beta} v_1}{\partial x_1^{\beta}} + \frac{\partial^{\beta} v_2}{\partial x_2^{\beta}}$ denotes a fractional β-order derivative of v_i along the x_i direction. The space $\mathcal{C}_0^l(\Omega, \mathbb{R}^2)$ represents the l-compactly supported continuous-integrable function space. When $\beta = 1$, the definition of TV^{β} coincides with that of TV.

3. Fractional-order total variation using Nash game

3.1. Problem formulation

Our model applies a non-local framework for our blind deconvolution problem to recover the image without blur and noise. Our work defines a combination of two techniques: the local method [1] and our proposal a non-local framework based on the work of Gilboa and Osher [7], in which: we split the original optimization into non-local and fractional order strategies to play a static game of complete information. We started with defined our functionals:

$$\min_{u} J_u(u,k) = \frac{1}{2}\|k \otimes u - z\|^2_{L^2(\Omega)} + \int_{\Omega} \alpha(x) \left|\nabla_{w-NL} u\right| dx + \frac{\delta}{2}\|u\|^2_{L^2(\Omega)}, \tag{17}$$

$$\min_{k} J_k(u,k) = \frac{1}{2}\|k \otimes u - z\|^2_{L^2(\Omega)} + \int_{\Omega} (1-\alpha(x))|\nabla^{\beta} k| \, dx. \tag{18}$$

Our objective is to engage in a competition involving two players following this structure:

- The first player utilizes the blurred image as a strategy to minimize (17).
- The strategy employed by the second player involves utilizing the kernel to minimize (18).
- Both players act simultaneously and iteratively.
- The objective is for both players to refine their strategies to achieve the optimal solution iteratively.

The goal is to demonstrate the existence and uniqueness of a solution (u^*, k^*) that minimizes both $J_u(u,k)$ and $J_k(u,k)$).

3.2. Analysis of our proposed method

This approach enhances the robustness of image restoration by leveraging the synergistic benefits of blind deconvolution, which addresses the convolution process, and fractional-order total variation regularization, which effectively reduces image blur while preserving more details and edges. This study presents a novel approach proposing a Nash equilibrium-based framework for Fractional-Order Total Variation (FOTV) as follows:

$$\min_{u,k} J(u,k) = \frac{1}{2}\|k \otimes u - z\|^2_{L^2(\Omega)} + \int_{\Omega} \alpha(x) \left|\nabla_{w-NL} u\right| dx + \int_{\Omega} (1-\alpha(x))|\nabla^{\beta} k| dx + \frac{\delta}{2}\|u\|^2_{L^2(\Omega)}, \tag{19}$$

where ∇^{β} represents the β-order gradient operator $(1 \leqslant \beta \leqslant 2)$, the non-local gradient $(\nabla_w u)(x) \colon \Omega \to \Omega$ is defined as follows:

$$(\nabla_{w-NL} u)(x,y) := (u(y) - u(x))\sqrt{w(x,y)}, \quad x, y \in \Omega \tag{20}$$

and $|\nabla^{\beta} k| = \sqrt{(\nabla_x^{\beta} k)^2 + (\nabla_y^{\beta} k)^2}$.

We resolve the functionals using the first-order optimality conditions:

$$\frac{\partial J_{u-NL}(k)}{\partial u} = k(-x,-y) \otimes (k \otimes u - z) - \nabla\alpha(x) \cdot \frac{\nabla_{w-NL}(u)}{|\nabla_{w-NL}(u)|} + \delta \cdot u = 0 \quad x \in \Omega, \tag{21}$$

$$\frac{\partial J(k)}{\partial k} = u(-x,-y) \otimes (u \otimes k - z) - (\nabla_x^{\beta})^{\mathrm{T}} \left[(1-\alpha(x)) \frac{\nabla_x^{\beta} k}{\sqrt{(\nabla^{\beta} k)^2 + \varepsilon^2}} \right] = 0 \quad x \in \Omega. \tag{22}$$

Incorporating $\alpha(x)$ as a spatially and scale adaptive function,

$$\frac{\partial J_{u-NL}(u)}{\partial u} = k(-x,-y) \otimes (k \otimes u - z)$$

$$-\int_{\Omega}\alpha(x)(u(y)-u(x))w(x,y)\left(\frac{1}{|\nabla_{w-NL}u|(x)}+\frac{1}{|\nabla_{w-NL}u|(y)}\right)dy+\delta\cdot u, \tag{23}$$

$$\frac{\partial J(k)}{\partial k}=u(-x,-y)\otimes(u\otimes k-z)-\left(\nabla_x^{\beta}\right)^{\mathrm{T}}\left[(1-\alpha(x))\frac{\nabla_x^{\beta}k}{\sqrt{(\nabla^{\beta}k)^2+\varepsilon^2}}\right]=0\quad x\in\Omega. \tag{24}$$

With $w(x,y)$ is a weighted function that presents the affinity between pixels based on image features (e.g. gray level value, edge indicator, dominant frequency, dominant direction, etc), the weight is defined generally by

$$w(x,y)=\begin{cases} g(Ff(x),Ff(y)) & \text{if } y\in\Omega_w(x),\\ 0 & \text{otherwise,}\end{cases}$$

where

$$g(Ff(x),Ff(y))=\exp\left\{-\left(\frac{\|Ff(x)-Ff(y)\|_2^a}{h}\right)^2\right\}, \tag{25}$$

$Ff(x)(u)=f(x)\in Bx$, where Bx is a patch centered at x, $\Omega_w(x)=\Omega$.

Solving these fractional differential equations simultaneously through an iterative method enables us to derive the optimal solution and approximate the deblurred image.

3.3. Algorithm Nash equilibrium

It is generally difficult to determine the optimal u and k simultaneously; a commonly used technique is alternating minimization, that alternatively updates one variable while keeping the other fixed. The Nash equilibrium is computed by the following decomposition algorithm.

Algorithm 1 Nash Equilibrium Algorithm for FOTV.

Input: Initial values $u^{(0)}$, $k^{(0)}$; Tolerance $\varepsilon>0$; Maximum iterations N
Output: Updated values $u^{(n)}$, $k^{(n)}$
Initialize $n\leftarrow 0$
while not converged and $n<N$
  Phase 1: Update u:
  $u^{(n+1)}\leftarrow\arg\min_u J_u(u,k^{(n)})$
  Phase 2: Update k:
  $k^{(n+1)}\leftarrow\arg\min_k J_k(u^{(n+1)},k)$
  Check convergence:
  if $\|u^{(n+1)}-u^{(n)}\|<\varepsilon$ **and** $\|k^{(n+1)}-k^{(n)}\|<\varepsilon$ **then**
    Convergence flag $\leftarrow$ `true`
  else
    Convergence flag $\leftarrow$ `false`
  Increment n by 1

4. Numerical experiments

In this section, we present the numerical results obtained from applying fractional-order total variation for image deblurring and compare our method with alternative approaches through two tests. We utilize standard images with varied fractional-order values to assess the effectiveness of our model.

To measure performance, we utilize the Peak Signal-to-Noise Ratio (PSNR) metric, the Structural Similarity Index Measure (SSIM), and the Improvement in Signal-to-Noise Ratio (ISNR). Our algorithm, based on the concept of total fractional variation, consistently outperforms conventional methods across a wide range of applications, demonstrating superior accuracy and precision.

In Test 1, we evaluate our approach against the improved Perona and Malik (IP-M) model proposed by Perona et al. [19], the fourth-order (F-O) PDE model introduced by You et al. [20], the improved fourth-order (IF-O) PDE model proposed by Hajiaboli et al. [21], the Rudin–Osher–Fatemi (ROF) model by Rudin et al. [2], and the fractional order total variation (FOTV) denoising algorithm. The standard images used in this test include Lena and Barbara (both sized at 512×512 pixels) and

Peppers (sized at 256 × 256 pixels). These images are subjected to Gaussian noise (at levels 10, 20, and 30) and a Gaussian blur kernel of size 3, with β set to 1.2 (as detailed in Table 1).

Table 1. Our result compared with some fractional order methods with gaussian noise 10, 20, 30.

Image	σ	IP-M	F-O-PDE	IF-O-PDE	ROF	$TV_2^\beta L^2$	Our-Method
Barbara	10	31.2427	29.3776	29.3777	31.0871	31.9791	**38.0261**
	20	26.6231	24.8155	24.8156	26.8212	26.9798	**36.3326**
	30	24.4496	22.9267	22.9273	24.7415	24.8166	**34.3686**
Lena	10	33.6393	31.3776	31.5442	33.8378	34.7437	**37.7452**
	20	29.7665	27.8080	24.8156	27.8098	31.4387	**36.7909**
	30	27.4437	26.0883	22.9273	26.1019	29.6095	**35.6760**
Peppers	10	33.6967	31.8199	31.8205	33.8715	**33.9328**	32.0172
	20	30.0275	28.0437	28.0457	30.1768	0.4965	**32.6416**
	30	27.4982	26.1613	26.1694	28.2689	28.8305	**31.8039**

In Test 2, we compare our method with ROF, Li et al. [22], FOTV, and Golbaghi et al. [23]. Using four standard images: Boat (512 × 512 pixels) and Cameraman, and Peppers (256 × 256 pixels), we again apply Gaussian noise (at levels 15 and 25) and a Gaussian blur kernel of size 3, with various β values (results are presented in Table 2).

Table 2. Our result compared with some fractional order methods with gaussian noise 15, 25.

Image	σ	ROF	Li [22]	Kazemi [23]	FOTV	$\beta = 1.2$	$\beta = 1.4$	$\beta = 1.6$	$\beta = 1.8$
Boat	15	34.4135	35.4193	35.8691	35.5267	**36.6882**	36.3396	36.3885	36.4989
Cameraman	15	28.4928	28.6568	29.4564	29.2562	**31.4537**	31.0828	31.1706	31.4220
Peppers	15	27.8284	27.3912	28.2503	27.9234	28.2503	**28.3451**	28.1105	27.8713
Boat	25	25.1717	26.1105	26.3206	26.2016	35.3350	35.6500	**36.8521**	36.7034
Cameraman	25	24.7547	25.9211	25.2113	25.4810	**30.9349**	30.9125	30.6907	30.6585
Peppers	25	24.2375	27.7213	26.9012	26.8215	26.9012	26.9667	**26.9719**	26.9390

a ***b*** ***c***

Fig. 1. Tests images, (***a***) The sharp image of Barbara, (***b***) The blurred image with gaussian noise 10 and gaussian blur kernel 3 and β=1.2, (***c***) The restored image using our method.

a ***b*** ***c***

Fig. 2. Tests images, (***a***) The sharp image of Barbara, (***b***) The blurred image with gaussian noise 20 and gaussian blur kernel 3 and $\beta = 1.2$, (***c***) The restored image using our method.

In these numerical results, the effectiveness of our algorithm, based on the concept of total fractional variation, stands out significantly. It consistently outperforms conventional methods, highlighting its potential to greatly enhance accuracy and precision across a wide array of applications. By incorporating the notion of fractional variation, our algorithm converges to a solution of vital importance, showcasing its superiority when compared to existing methods.

Table 1 presents a comparative analysis between our proposed method and five conventional methods. Our approach exhibits superior efficiency, particularly concerning the Barbara and Lena images, as evidenced by the evaluation using PSNR.

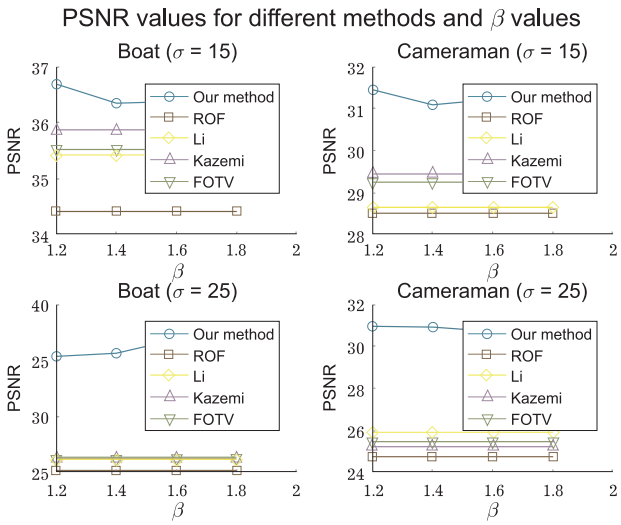

Fig. 3. This plot compares the PSNR values of different methods applied to two images (Boat, Cameraman) with Gaussian noise levels $\sigma = 15$ and $\sigma = 25$. The methods compared are ROF, Li, Kazemi, FOTV, and several versions of the "Our Method" parameterized by β values (1.2, 1.4, 1.6, 1.8).

This visualization facilitates a comparative analysis of the effectiveness of various denoising and deblurring methods across different images and noise levels. It specifically highlights the β value that yields the highest PSNR for our method, thereby indicating its optimal parameter setting for superior deblurring efficiency (Figure 3).

Table 2 provides a comparative analysis of PSNR measurements across fractional orders of β (1.2, 1.4, 1.6, 1.8). Our proposed method shows optimal performance with beta values between 1.2 and 1.6.

a ***b*** ***c***

Fig. 4. Tests images, (***a***) The sharp image of Lena, (***b***) The blurred image with gaussian noise 10 and gaussian blur kernel 3 and $\beta = 1.2$, (***c***) The restored image using our method.

a ***b*** ***c***

Fig. 5. Tests images, (***a***) The sharp image of Lena, (***b***) The blurred image with gaussian noise 20 and gaussian blur kernel 3 and $\beta = 1.2$, (***c***) The restored image using our method.

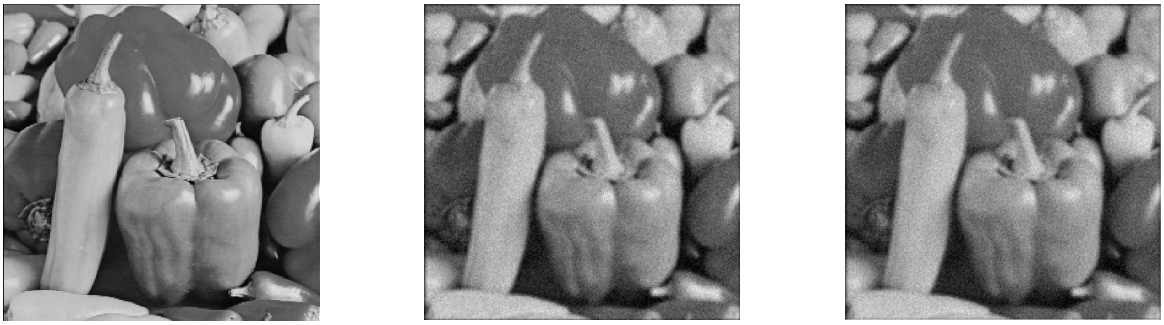

a ***b*** ***c***

Fig. 6. Tests images, (***a***) The sharp image of Peppers, (***b***) The blurred image with gaussian noise 10 and gaussian blur kernel 3 and $\beta = 1.2$, (***c***) The restored image using our method.

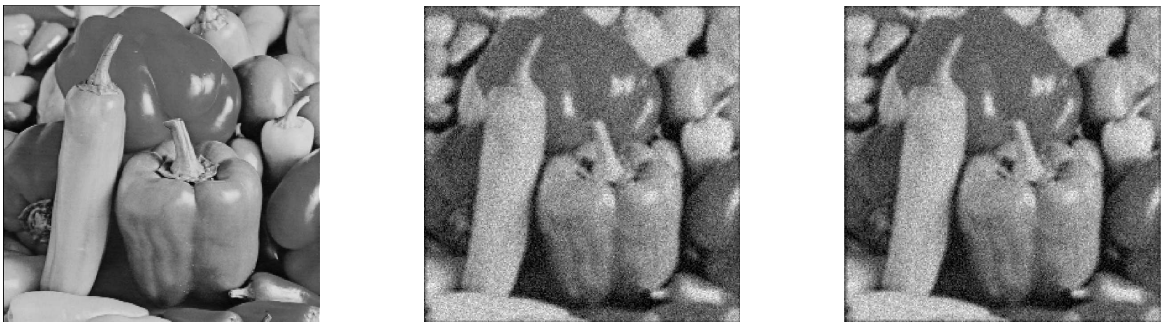

a ***b*** ***c***

Fig. 7. Tests images, (***a***) The sharp image of Peppers, (***b***) The blurred image with gaussian noise 20 and gaussian blur kernel 3 and $\beta = 1.2$, (***c***) The restored image using our method.

a ***b*** ***c***

Fig. 8. Tests images, (***a***) The sharp image of Boat, (***b***) The blurred image with gaussian noise 15 and gaussian blur kernel 3 and $\beta = 1.2$, (***c***) The restored image using our method.

a ***b*** ***c***

Fig. 9. Tests images, (***a***) The sharp image of Boat, (***b***) The blurred image with gaussian noise 25 and gaussian blur kernel 3 and $\beta = 1.4$, (***c***) The restored image using our method.

a ***b*** ***c***

Fig. 10. Tests images, (***a***) The sharp image of Boat, (***b***) The blurred image with gaussian noise 15 and gaussian blur kernel 3 and $\beta = 1.6$, (***c***) The restored image using our method.

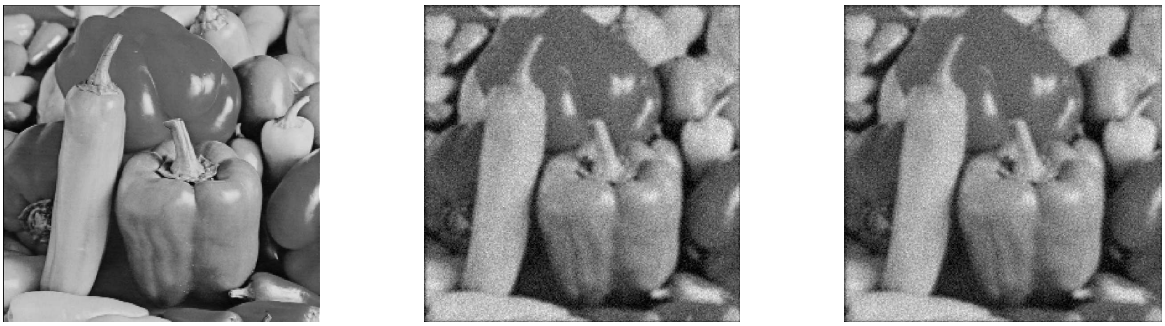

a ***b*** ***c***

Fig. 11. Tests images, (***a***) The sharp image of Peppers, (***b***) The blurred image with gaussian noise 15 and gaussian blur kernel 3 and $\beta = 1.4$, (***c***) The restored image using our method.

5. Conclusion

The proposed methodology integrates fractional-order total variation with Nash game principles to advance the efficiency of image deblurring and eliminate the staircase artifacts typically encountered in image restoration.

By incorporating fractional-order total variation, the method adeptly balances image smoothness with edge preservation. This integration is crucial for maintaining sharp image details while effectively reducing artifacts such as staircase effects.

Additionally, the application of Nash game principles introduces a competitive optimization framework that enhances the deblurring process through the consideration of interactions between different image regions. This localized approach leverages the intrinsic characteristics of the image to refine accuracy in restoration.

In summary, the synthesis of fractional-order total variation and Nash game principles within our method presents a robust solution for image deblurring. This convergence not only augments efficiency but also produces high-quality restored images devoid of undesirable staircase artifacts.

[1] Meskine D., Moussaid N., Berhich S. Blind image deblurring by game theory. NISS'19: Proceedings of the 2nd International Conference on Networking, Information Systems & Security. 31 (2019).

[2] Rudin L. I., Osher S., Fatemi E. Nonlinear total variation based noise removal algorithms. Physica D: Nonlinear Phenomena. **60** (1–4), 259–268 (1992).

[3] Karami F., Meskine D., Sadik K. Nonlocal total variation system for the restoration of textured images. International Journal of Computer Mathematics. **98**, 1749–1768 (2021).

[4] Kang M., Jung M. Simultaneous image enhancement and restoration with non-convex total variation. Journal of Scientific Computing. **87**, 83 (2021).

[5] Aboulaich R., Habbal A., Moussaid N. Optimisation multicritère : Une approche par partage des variables. Revue Africaine de la Recherche en Informatique et Mathématiques Appliquées. **13**, 77–89 (2010).

[6] Nasr N., Moussaid N., Gouasnouane O. A game theory approach for joint blind deconvolution and inpainting. Mathematical Modeling and Computing. **10** (3), 674–681 (2023).

[7] Gilboa G., Osher S. Nonlocal linear image regularization and supervised segmentation. Multiscale Modeling and Simulation. **6** (2), 595–630 (2007).

[8] Buades A., Coll B., Morel J. M. A review of image denoising algorithms, with a new one. SIAM Multiscale Modeling and Simulation. **4** (2), 490–530 (2005).

[9] Li R., Zhang X. Adaptive sliding mode observer design for a class of T-S fuzzy descriptor fractional order systems. IEEE Transactions on Fuzzy Systems. **28** (9), 1951–1960 (2020).

[10] Zhang X., Dong J. LMI criteria for admissibility and robust stabilization of singular fractional-order systems possessing poly-topic uncertainties. Fractal Fractional. **4** (4), 58 (2020).

[11] Zhang X., Yan Y. Admissibility of fractional order descriptor systems based on complex variables: An LMI approach. Fractal Fractional. **4** (1), 8 (2020).

[12] Yang Q., Chen D., Zhao T., Chen T. Fractional calculus in image processing: A review. Fractional Calculus and Applied Analysis. **19**, 1222–1249 (2016).

[13] Zhou L., Tang J. Fraction-order total variation blind image restoration based on L^1-norm. Applied Mathematical Modelling. **51**, 469–476 (2017).

[14] Zhang Y., Zhang W., Lei Y., Zhou J. Few-view image reconstruction with fractional-order total variation. Journal of the Optical Society of America A. **31** (5), 981–995 (2014).

[15] Zhang J., Wei Z. Fractional Variational Model and Algorithm for Image Denoising. 2008 Fourth International Conference on Natural Computation. 524–528 (2008).

[16] Zhou L., Zhang T., Tian Y., Huang H. Fraction-Order Total Variation Image Blind Restoration Based on Self-Similarity Features. IEEE Access. **8**, 30436–30444 (2020).

[17] Yan S., Ni G., Liu J. A fractional-order regularization with sparsity constraint for blind restoration of images. Inverse Problems in Science and Engineering. **29** (13), 3305–3321 (2021).

[18] Zhang J., Chen K. A total fractional-order variation model for image restoration with nonhomogeneous boundary conditions and its numerical solution. SIAM Journal on Imaging Sciences. **8** (4), 2487–2518 (2015).

[19] Perona P., Malik J. Scale-space and edge detection using anisotropic diffusion. IEEE Transactions on Pattern Analysis and Machine Intelligence. **12** (70, 629–639 (1990).

[20] You Y. L., Kaveh M. Fourth-order partial differential equations for noise removal. IEEE Transactions on Image Processing. **9** (10), 1723–1730 (2000).

[21] Hajiaboli M. A self-governing fourth-order nonlinear diffusion filter for image noise removal. IPSJ Transactions on Computer Vision and Applications. **2**, 94–103 (2010).

[22] Li F., Shen Ch., Fan J. Image restoration combining a total variational filter and a fourth-order filter. Journal of Visual Communication and Image Representation. **18** (4), 322–330 (2007).

[23] Kazemi Golbaghi F., Rezghi M., Eslahchi M. R. A Hybrid Image Denoising Method Based on Integer and Fractional-Order Total Variation. Iranian Journal of Science and Technology, Transactions A: Science. **44**, 1803–1814 (2020).

Сліпе усунення розмиття зображення за допомогою дробових похідних і повної варіації: підхід рівноваги Неша

Бергіч С., Мусаїд Н.

Університет Хасана II Касабланки, LMCSA, FST, Мохаммадія

Моделювання дробового порядку є життєздатним підходом для усунення властивих обмежень загальної варіації в задачах усунення розмиття зображення. Цей підхід досягається за рахунок дискретизації дробових похідних і демонструє значний прогрес у покращенні якості реконструйованих зображень. Спираючись на успіх нашої попередньої роботи зі сліпої деконволюції, де використано загальну варіацію на основі зображення для зменшення ефекту сходів, аналізуємо та тестуємо нову модель сліпого усунення розмиття на основі дробових похідних β-порядку за допомогою гри Неша. У цій грі використовується той самий тип гравців, кожен зі своєю стратегією пошуку оптимального рішення, як визначено в нашій попередній роботі. Крім того, порівнюємо наш запропонований метод з класичними методами та методами дробового порядку з різними параметрами β. Наші чисельні результати демонструють, що наш метод досягає вищої ефективності та кращої якості зображення порівняно з існуючими методами реконструкції.

Ключові слова: *сліпе зображення; зменшення розмитості зображення; похідні дробового порядку; загальна варіація; рівновага Неша.*

AUTHOR INDEX OF VOL. 11, No. 4 (2024)

INSTRUCTIONS TO THE AUTHORS

Submission: Submission of a manuscript to the Editorial Board implies that the work described has not been published previously (except in the form of an abstract or as part of an academic thesis or e-preprint) and is not currently under consideration for publication elsewhere. A manuscript, written in English (up to 15 pages), should be prepared with the help of publishing system LaTeX (see Preparation of manuscript). The author's files (LaTeX+Artworks+PDF files united in one archive (zip-file)) with two hard copies of PDF-file (with supporting documentation for Ukrainian authors) are to be submitted to the Editorial Board on a CD disk or by e-mail. Electronic submission also implies the delivery of two hard copies to **the Editorial Board**:

Lviv Polytechnic National University
1 St. Yura square, room 127
79013, Lviv, Ukraine
e-mail: mmc@lpnu.ua

Preparation of manuscripts: The style files for manuscripts preparing may be obtained via the WWW (`http://science.lpnu.ua/mmc`) or e-mail by sending a message to `mmc@lpnu.ua` with subject: get templates. Instructions how to use style files are in the readme file. If for some reasons the authors do not have access to Internet, the manuscripts can be typesetted using standard LaTeX styles by placing in its preamble the following commands:

```
\documentclass[11pt]{article}
\textheight=240mm
\textwidth=170mm
```

Manuscripts must be arranged in the following order: the title of the article, the author's name/names and their affiliations, a short title of no more than 45 characters, an abstract (up to 150 words), up to six key words, 2010 MSC numbers, the text of the article, acknowledgments, appendices, references. Separately the contributors are asked to provide the title, the author's name/names and their affiliations, an abstract and key words in Ukrainian. Figures and tables should be included in the text where they are to be placed.

Artwork: Artworks should be prepared in a computer-readable form (EPS, PS or any black and white bitmap). Bitmapped graphics should have 600 or 300 dpi resolution.

References: References are to be numbered sequentially through the text and listed at the end of the paper using only roman font of the same size with pointing out the titles for books and for conference proceedings. A typical example of a reference list is:

```
\bibitem{Mittelbach} Mittelbach\;F., Goossens\;M., Braams\;J., Carlisle\;D.,
                     Rowley\;C. The \LaTeX\ Companion (Tools and Techniques
                     for Computer Typesetting).
                     Addison-Wesley Professional; 2nd edition (2004).

\bibitem{Oetiker} \verb"http://ctan.org/tex-archive/info/lshort/"

\bibitem{Burnside} Burnside\;W. A rapidly convergent series for $\log N!$
                   Messenger Math. \textbf{46}, 157 (1917).
```